Electronic Supplementary Information

Optically assembled droplet interface bilayer (OptiDIB) networks from cell-sized microdroplets

Mark S. Friddin, Guido Bolognesi, Yuval Elani, Nicholas J. Brooks, Robert V. Law, John M. Seddon, Mark A. A. Neil and Oscar Ces

1) Coverslip preparation

Glass coverslips 24 x 60 mm (VWR, UK) were solvent cleaned, dried and baked at 90˚C for 30 minutes. Sylgard 184 Silicone Elastomer Kit (Dow Corning, USA) was prepared using a 1:10 ratio of curing agent to bulk elastomer and spin-coated onto the glass coverslips at 3,000 RPM for 60 seconds. The resulting PDMS film was cured by baking the coverslip at 90˚C for 10 minutes. A well was created from a self-adhesive polyamide thermal interface pad (RS Components, UK).

2) Optical Setup

An inverted epi-fluorescence dual-carousel microscope (Nikon TE2000-U) combined with an optical trapping system was used for imaging and optical manipulation. The custom-built laser trapping optics of this set-up was originally designed for the simultaneous trapping of multiple particles by time-multiplexed optical tweezers, as described by Lanigan et al.[1] The linearly polarised beam from an Ytterbium fibre laser source (20W at 1070nm) was expanded using a pair of IR doublets in order to fill the 1280x1024 pixel display of a ferroelectric liquid crystal on silicon (FLCOS) spatial light modulator (SLM) (CRL-Opto SXGA-R-H1). The waist of the beam from the SLM was adjusted by means of a second pair of IR doublets in order to slightly overfill the back-aperture of 60x 1.4 N.A. oil immersion objective mounted on the inverted microscope. A IR dichroic mirror and a IR filter were inserted in the upper carousel of the microscope to direct the trapping beam towards the objective while preventing any beam reflection from reaching the CCD camera (ORCA-ER Hamamatsu). Two Nikon filter cubes (FITC and TRITC), inserted in the lower carousel, together with a mercury-fibre illuminator (Nikon Intensilight C-HGFIE) were used for imaging the droplets in fluorescence mode. The image acquisition process was controlled using a customised Labview (National Instruments Corp) interface. In this work, the simultaneous manipulation of multiple droplets was not required and a single optical trap was used instead. Two half-wave plates, placed one before and one after the SLM, were oriented so that the transmitted beam was no longer modulated by the SLM. Consequently, the latter acted as a simple mirror and the unmodulated (0^{th} order) beam was used to power the single optical trap. The optical manipulation of single droplets typically required a laser power of 150 mW at the back aperture of the objective. In order to drag a whole DIB network composed of several droplets (see section 6), laser powers up to 460 mW at the objective back aperture were used. This rather simple implementation of optical tweezers shows that no complicated optical set-up was required to construct complex 2D and 3D DIB networks.

To conclude, it is noted that since the optical transmittance of the objective is about 60%, a total laser power of about 90 mW at the sample is expected during operation. As a result, droplets were exposed to a maximum light intensity of $I_{MAX} = \frac{90\ \mathrm{mW}}{\pi d^2/4} \approx 20\ \mathrm{MW/cm^2}$ where $d \approx \frac{1070nm}{NA} \approx 750$ nm. Since each droplet was exposed to such light intensity only during manipulation, which typically required less than a minute, the energy dose delivered to each droplet was less than 5 J. Finally, for a 100 mW optical trap a laser-induced temperature increase in the range from 1 to 2 °C is expected. Under these conditions, any biological material encapsulated in the trapped droplets will not be damaged by the laser, thereby proving the potential of this platform for synthetic biology and drug screening applications.

3) Lipid Preparation

The desired amount of lipid was dissolved in chloroform inside a glass vile. The solvent was evaporated under a stream of nitrogen to leave a lipid film which was stored inside a vacuum desiccator overnight to remove any residual solvent. Lipid-out technique: The 1,2-diphytanoyl-sn-glycero-3-phosphocholine (DPhPC) lipid film was dissolved in tetradecane (Sigma-Aldrich, UK) to yield a final concentration of 5 mg/ml and placed in a standard benchtop ultrasonic bath at full power for 30 min. Lipid-in technique: To prepare lipid vesicles, the lipid film was re-suspended in the desired amount of buffer containing 2M sucrose to yield a final concentration of 1 mg/ml. Small unilamellar vesicles were formed either by sonication using a standard benchtop ultrasonic bath at full power for 60 min or by extrusion, where the lipid in buffer dispersion was freeze-thawed 5 times and passed 21 times through a polycarbonate filter with an average pore size of 100 nm. The fluorescent lipids used were NBD-PE [1,2-dipalmitoyl-sn-glycero-3-phosphoethanolamine-N-(7-nitro-2-1,3-benzoxadiazol-4-yl) (ammonium salt)] and Rh-PE [,2-dipalmitoyl-sn-glycero-3-phosphoethanolamine-N-(lissamine rhodamine B sulfonyl) (ammonium salt)]. These were imaged using FITC and TRITC filters respectively (green and yellow channels). Fluorescent lipids were present at 1 wt. %. All lipids were purchased from Avanti Polar Lipids (USA).

4) Microdroplet generation

Buffer containing 2M Sucrose, 500mM KCl, 25mM Tris-HCl, pH 8.0 was dispensed inside a volume of 5 mg/mL DPhPC in tetradecane at a ratio of 1:100 and aspirated using a pipette. The shear forces generated were sufficient to form a range of droplet sizes, the smallest of which were selected by taking a 30 µl sample from the top of the dispersion. The sample was loaded onto a PDMS coverslip and the process was repeated for additional droplet types.

5) 3D droplet manipulation

The surface of the PDMS coated coverslip was focused under a 60x 1.40 NA oil immersion objective and scanned for appropriately sized droplets using the XY motorised microscope stage. A live video feed allowed for adequately sized droplets to be visualised/selected and fluorescent micrographs were obtained to discriminate between the droplet types where necessary. The motorised stage was used to target the laser toward the desired droplet and the laser was turned on (typical power = 0.5W). An initial, subtle movement in the droplet toward the centre of the laser beam indicated that the droplet was trapped. Droplets were typically lifted off the PDMS surface by changing the focus of the objective (and therefore the laser) in the Z direction and then manipulated in the X and Y directions using the motorised stage to a dedicated region of the coverslip for DIB network assembly. It was noted that smaller droplets were easier to trap and manipulate at 0.5W compared to larger droplets. This process was repeated to collect the desired number of droplets and droplet types for OptiDIB formation and network assembly.

6) OptiDIB formation

Prior to OptiDIB formation, the desired droplets were selected and placed in close proximity to each other (Fig. 1A). One of the two droplets was then trapped with the laser and moved into contact with the other (Fig. 1B-C). The second droplet was pushed slightly by the trapped droplet to ensure that contact was made and the droplets were left for a few seconds for the bilayer to form. In this case, OptiDIB formation is inferred by the interdroplet bond that subsequently forms. This is illustrated by the ability to drag the second droplet via the first in the X (Fig. 1D), Y (Fig. 1E) and Z directions (Fig. 1F). It was sometimes found that the optical trap could also break the DIB by separating the droplets, but this was not repeatable and requires further investigation (data not shown).

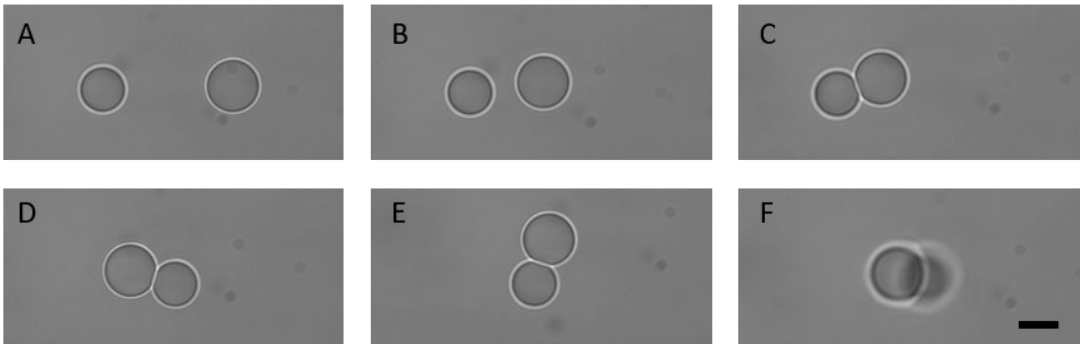

Fig. 1 OptiDIB formation and droplet manipulation in 3D. (A)-(C) One droplet is trapped with the laser and manipulated into contact with another. DIB formation is indicated by the ability to drag the second droplet via the first in the (D) X, (E) Y and (F) Z directions. Scale bar = 15 µm.

6) OptiDIB network formation

OptiDIB networks were assembled by adding additional droplets to an existing two droplet OptiDIB as described above. The resulting adhesion at the droplet interfaces was highlighted by the ability to drag the whole OptiDIB network in the X (Fig. 2A), Y (Fig. 2B) and Z (Fig. 2C) directions by only trapping and manipulating one of the droplets. When the laser was turned off, the droplet network fell to the bottom of the well (Fig. 2D).

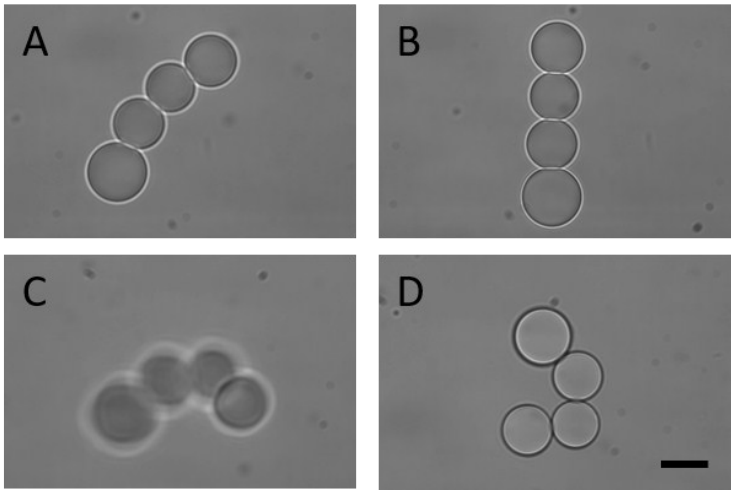

Fig. 2 OptiDIB network manipulation in 3D. (A) The interconnected droplet chain is dragged in the X and (B) Y direction by the leading (top) droplet. (C) The droplet chain also remains intact when dragged in the Z direction by the leading droplet. (D) The droplets fall to the bottom of the well when the laser is turned off. Scale bar = 15 µm.

7) Interdroplet exchange of calcium ions

The additional data referenced in the main article for droplet is shown in Fig. 3A. The data from the control used in the article is repeated in Fig. 3B for reference. The change in fluorescence intensity of the droplets containing the calcium sensitive dye Fluo-4 (Life Technologies, UK) is plotted for both samples in in Fig. 3C, in addition to the OptiDIB shown in the main text (red line, circles) . The data shows a ca. 1.5x increase in signal over 10 minutes for the droplet in Fig. 3A, while no increase in signal was observed for the control droplet. The increasing fluorescent signal is attributed to the interdroplet exchange of calcium ions via αHL nanopores (Sigma-Aldrich, UK) inserted into the DIB. The bigger droplets in this example, namely the increase in bilayer area, most likely accounts for the larger signal observed compared to the data shown in the main article. Fig. 3D confirms that no droplet shrinkage was observed in any of the measured droplets.

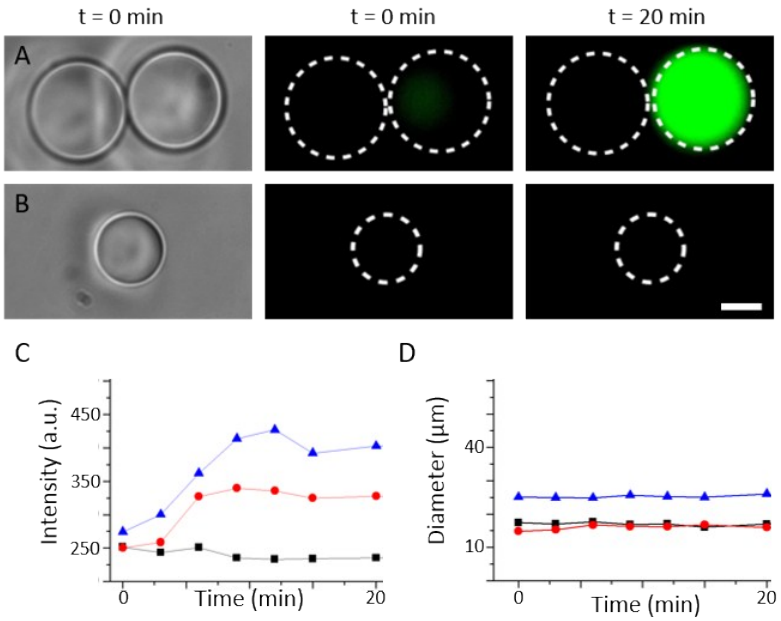

Fig. 3 Interdroplet exchange of calcium ions through αHL pores inserted into DIBs. (A) Droplets containing 12 µM αHL in 2M sucrose and either 500 mM $CaCl_2$ (left) or 200 µM EDTA and 5.3 µM Fluo-4 (right) were manipulated into contact and imaged. The figure shows a brightfield micrograph obtained at the beginning of the experiment next to brightfield/fluorescent composites taken at the beginning and end of the measurement. (B) The control droplet (as shown in the main article) containing αHL, EDTA and Fluo-4 in buffer containing 2M sucrose was imaged simultaneously. Scale bar for all micrographs = 10 µm (C) A plot showing the change in fluorescent intensity of the dye containing droplet in part (A) (black line, squares), part (B) (blue line, triangles) and the droplet shown in the main article (red line, circles) for the duration of the 20 min experiment. (D) Plot showing the change in droplet diameter of the dye containing droplets during the 20 min experiment. The symbols relate to the same samples in (C).

8) Characteristic diffusion time of calcium ions in water droplets:

In order to estimate the characteristic time for calcium ions to diffuse across a droplet, we need to calculate the diffusion coefficient D of the ions in the sucrose aqueous solution. According to the Stokes-Einstein (SE) relation, the coefficient D is inversionally proportional to the dynamic viscosity η of the liquid phase. However, both experimental and computer simulation studies[4] have shown that for small solute particles (like ions) the prediction of the SE relation underestimates the actual value of the diffusion coefficient. Consequently, we can use the simple SE relation to determine an upper limit for the characteristic diffusion time of the calcium ions. The diffusion coefficient of calcium ions in DI water is $D = 0.07 \cdot 10^{-8} \mathrm{m}^2/\mathrm{s}$. Since the dynamic viscosity of a 2M sucrose solution is ca 28 times the dynamic viscosity of DI water, the coefficient D is reduced to $2.5 \cdot 10^{-11} \mathrm{m}^2/\mathrm{s}$ for calcium ions in the sucrose solution. As a result, the time required for the ions to diffuse across a 20 µm diameter droplet is given by

$$t = \frac{(20\ \mu\mathrm{m})^2}{2 \text{ x } 2.5 \cdot 10^{-11} \mathrm{m}^2 \mathrm{s}^{-1}} \approx 8\ \mathrm{s} \qquad (2)$$

The characteristic diffusion time is hence negligible compared to the time lapse between DIB formation and plateauing of the fluorescent signal in the bioassay (Fig 3C).

References

1. P. M. P. Lanigan, I. Munro, E. J. Grace, D. R. Casey, J. Phillips, D. R. Klug, O. Ces and M. A. A. Neil, *Biomed. Opt. Express*, 2012, **3**, 1609-1619.
2. K. König, *Histochemistry and Cell Biology*, 2000, **114**, 79-92.
3. K. C. Neuman, E. H. Chadd, G. F. Liou, K. Bergman and S. M. Block, *Biophysical Journal*, **77**, 2856-2863.
4. S. Acharya, M. K. Nandi, A. Mandal, S. Sarkar and S. M. Bhattacharyya, *The Journal of Physical Chemistry B*, 2015, **119**, 11169-11175.